solidified alloys.

	% Eutectic phase
7	51.0 ± 1.07
	52.1 ± 2.14
	41.9 ± 1.04
	26.8 ± 1.72
7	16.04 ± 1.27
	17.6 ± 1.63

ives a reasonably good quantitative
ned during solidification. These
thod that can be used to predict the
he Pb-77.5 % Sn alloy have some
sistency to improve the prediction

oconstituents formed during the
accurate for the calculation of the
an on-line tool. It is necessary to
surements obtained by quantitative

support and A. Amaro, I. Beltran

7.
p. 505.
7), p. 349.
nd J.H. Sokolowski: Trans. AFS,

1988), p. 3057
455.

Materials Science Forum Vol. 509 (March 2006) pp. 153-158
online at http://www.scientific.net

Newton Thermal Analysis of Gray and Nodular Eutectic Cast Iron

M.R.Chavez[1,a], A.Amaro[1,a], C.Flores[1,a], A.Juarez[2,b],C. González-Rivera[1,a]

[1]Departamento de Ingeniería Metalúrgica, Edif. "D", Facultad de Química, UNAM, Circuito Exterior S/N, Cd. Universitaria, 04510, México D.F., México.

[2]CIATEQ A. C. Calz. Del Retablo 150, Col. Fovissste, 76150 Queretaro Qro., México.

[a] carlosgr@servidor.unam.mx , [b] ajuarez@ciateq.mx

Keywords: Newton Thermal Analysis, Eutectic Nodular Iron, Eutectic Gray Iron, Solidification.

Abstract. The purpose of this work is to analyze the capability of Newton Thermal Analysis (NTA) to detect differences of the solidification kinetics between eutectic gray and ductile irons obtained from the same base alloy. The NTA experimental output has been analyzed with a simple micro-macro modeling approach. The outcome of this work suggests that NTA has a good potential as a qualitative tool to characterize the solidification kinetics of alloys.

Introduction

Computer aided cooling curve analysis (CACCA), such as Fourier Thermal Analysis (FTA) [1-3] Newton Thermal Analysis (NTA) [4-6], are valuable tools that give a deeper understanding of the solidification of cast alloys. The interest on these techniques relies on the successful identification of several cooling curve parameters by conventional cooling curve analysis (CCA). This allows the prediction of the microstructure of cast products. Another reason is the need to develop more elaborated cooling curve data processing methods in order to gain a better understanding of solidification and a closer control of the melt quality before pouring.

CACCA is based on the fact that the phase transformations and microstructure formation kinetics that occur during solidification and cooling of a cast are intimately linked with the cooling curves obtained. Accordingly, CCA is commonly applied to control the grain size and to modify the eutectic microconstituent of Al-Si alloys [7], and to control the chemical composition (carbon and silicon content) of cast irons [8].

The NTA methodology has been described in detail elsewhere [1, 4, 5]. It analyzes a cooling curve that is obtained with a thermocouple located at the thermal centre of a cast. NTA calculations are performed on the first derivative of that curve. In the classical version of this method [4], the times of start and end of solidification are located. The zero baseline curve is obtained from an exponential interpolation between these points. Integration of the area between the cooling curve and the zero baseline curve gives relevant information of the solidification kinetics.

It has been argued that the NTA method is not reliable to make quantitative predictions of the latent heat of solidification due to the arbitrary nature of the zero curve calculation [5,9]. However, it has potential as an approximate, qualitative method to study the solidification kinetics of several cases of metallurgical interest [10-12].

The capability of NTA to detect changes of the solidification kinetics can be recognized by applying it to study the solidification kinetics of melts that have similar chemical composition and thermophysical properties, but that differ in the solidification mechanism.

The most important microstructural difference between eutectic gray and ductile irons is the morphology of the graphite. This difference reflects a change of the solidification mechanisms and kinetics. Eutectic gray iron solidifies by an irregular, cooperative growth of graphite lamellae and austenite. These phases form eutectic equiaxial cells that grow until the end of solidification [13,14]. The solidification of eutectic nodular iron is not completely understood [15], although it is accepted that the growth of graphite during the solidification is restricted by diffusion of C from the

liquid to the graphite nodules through intermediate layers of austenite [16,17].

The purpose of this work is to determine the capability of NTA to detect the differences in solidification kinetics of eutectic gray and ductile irons obtained from the same base alloy in order to explore its use as a qualitative tool to characterize the solidification kinetics.

Experimental Procedure

A base alloy with the chemical composition shown in Table 1 was produced by melting 100 kg of gray iron scrap in an induction furnace and poured into ingots. Near eutectic gray iron was produced using the base alloy, ferroalloys and an inoculant (75 % Ferro-silicon powder). Nodular iron was prepared using a 6% Magnesium nodulizer and low carbon steel scrap; the nodularization was obtained using the sandwich method. The chemical composition of the molten metal was measured by emission spectrometry. It was adjusted with coke and ferro-silicon in order to obtain a carbon equivalent (C. E.) close to the eutectic composition. The chemical compositions of the gray iron and the nodular iron are given in Table 1. The two alloys had a near eutectic composition.

Table 1. Chemical compositions of the base alloy, the gray iron and the nodular iron (in wt. %)

Alloy	C	Si	Mn	P	S	Mg	Fe
Base	3.8	1.8	0.3	0.06	0.12	<0.005	Bal.
Gray Iron	4.2	2.1	0.4	0.05	0.18	<0.005	Bal.
Nodular Iron	4.1	2.1	0.5	0.03	0.06	0.047	Bal.

Predetermined quantities of the molten alloys were poured with minimum turbulence in a cylindrical sand mold thermally isolated at the top and bottom. A silicate/CO_2 bonded sand mold, with a 5 cm inner diameter, 7.5 cm height and 3 cm wall thickness was used in all cases. In order to enhance the experiments reproducibility, the molds were positioned in molding boxes and surrounded with silica sand before pouring. A type K thermocouple was always positioned at 30 mm from the bottom of the mold centre to ensure reproducibility of the analysis. The thermocouple tips were protected with a zirconia cover. The cooling curves were obtained by recording the temperature variation as a function of time with an Iotech Tempscan 1100 data acquisition system. The results were obtained by triplicate for each alloy. The solidified rods were cut in halves. One cross section was prepared with standard metallographic methods. The graphite morphology was determined in an optical microscope.

Results and Discussion

Fig.1 shows the cooling curves and the NTA solidification rate typically associated with the cases under study. It can be seen that the solidification kinetics obtained from the NTA numerical processing of the cooling curves show a marked difference between the gray and nodular cast irons studied. Nodular iron shows a solidification rate (df_s/dt) that increases in the first stages of solidification, reaches a maximum and decreases progressively as solidification proceeds. Gray iron shows an increasing solidification rate at the beginning of the solidification, followed by an almost constant solidification rate during most of the solidification process, which ends with a steep decrease at the end of solidification.

Microstructures of the experimental specimens are shown in Fig. 2. Here, it can be seen that the nodular iron has spherulitic graphite. The gray iron has typical carbon flakes.

At this stage of the work it was clear that the NTA method was capable of detecting differences in solidification kinetics between the two types of iron alloys. These differences and the observed changes in microstructure suggest a change of the solidification mechanisms operating in both alloys. However, in order to generate more evidence to support that the observed changes in NTA solidification kinetics were linked to changes in solidification mechanisms, a simple heat transfer -

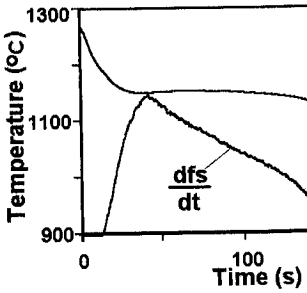

(a)

Figure 1. Experimental Co
(a)

(a)

Figure 2. Microstru

solidification kinetics (HT
mechanisms of interest and
was used to generate coolin
curves were numerically pr
the experimental results.

The HT-SK model was b
gradients exist throughout t
heat extraction is primarily
the specimen [18]. A lumpe

$$Cp^V \frac{dT}{dt} = L_S \frac{dfs}{dt} - \frac{h_\infty (T -$$

Where Cp^V is the volumetri
of solidification (J/m^3), dfs/
T the instantaneous tempera
specimen (m). Before and
obtained from the numerica

$$h_\infty = -Cp^V \frac{M}{(T - T_\infty)} \frac{dT}{dt}$$

of austenite [16,17].
lity of NTA to detect the differences in
tained from the same base alloy in order
lidification kinetics.

le 1 was produced by melting 100 kg of
o ingots. Near eutectic gray iron was
(75 % Ferro-silicon powder). Nodular
w carbon steel scrap; the nodularization
composition of the molten metal was
ke and ferro-silicon in order to obtain a
The chemical compositions of the gray
s had a near eutectic composition.

y iron and the nodular iron (in wt. %)

	S	Mg	Fe
	0.12	<0.005	Bal.
	0.18	<0.005	Bal.
	0.06	0.047	Bal.

ured with minimum turbulence in a
m. A silicate/CO_2 bonded sand mold,
kness was used in all cases. In order to
positioned in molding boxes and
ocouple was always positioned at 30
lity of the analysis. The thermocouple
ves were obtained by recording the
mpscan 1100 data acquisition system.
lidified rods were cut in halves. One
thods. The graphite morphology was

e typically associated with the cases
obtained from the NTA numerical
ween the gray and nodular cast irons
at increases in the first stages of
as solidification proceeds. Gray iron
olidification, followed by an almost
process, which ends with a steep

Fig. 2. Here, it can be seen that the
arbon flakes.
vas capable of detecting differences
These differences and the observed
ion mechanisms operating in both
that the observed changes in NTA
chanisms, a simple heat transfer -

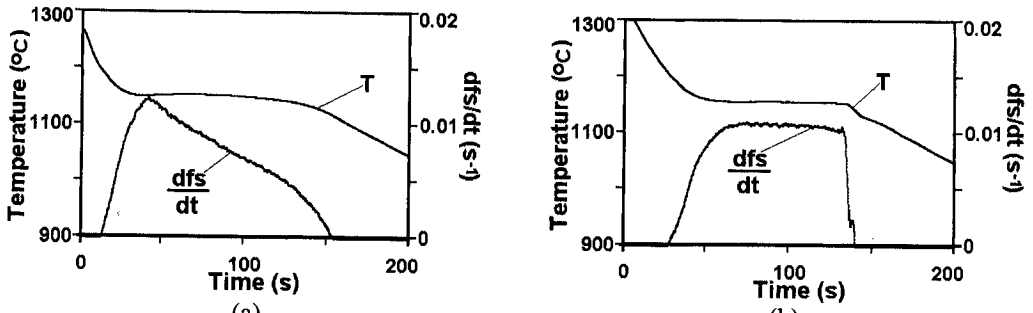

Figure 1. Experimental Cooling curve (T) and NTA solidification rate (dfs/dt) corresponding to (a) Eutectic nodular iron; (b) Eutectic gray iron.

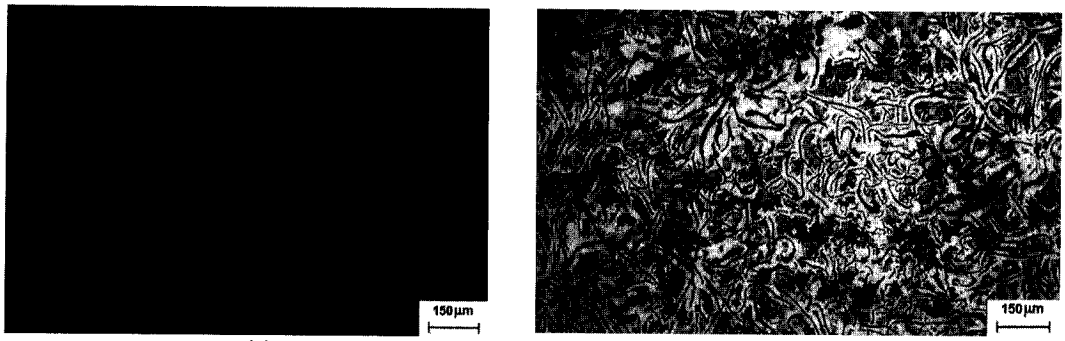

Figure 2. Microstructures of (a) Eutectic nodular iron, and (b) Eutectic gray iron.

solidification kinetics (HT-SK) model was implemented to simulate the two solidification mechanisms of interest and the cooling conditions present during the experimentation. This model was used to generate cooling curves corresponding to the experimental cooling conditions. These curves were numerically processed by NTA to use them as a reference during the interpretation of the experimental results.

The HT-SK model was based on a lumped heat balance considering that negligible temperature gradients exist throughout the thermal analysis of the specimen during cooling so that the rate of heat extraction is primarily determined by the thermal resistance associated with the boundary of the specimen [18]. A lumped heat balance of the probe can be written as follows:

$$Cp^{V}\frac{dT}{dt} = L_S\frac{dfs}{dt} - \frac{h_\infty(T-T_\infty)}{M} \qquad (1)$$

Where Cp^V is the volumetric heat capacity (J/m^3°C), dT/dt the cooling rate (°C/s), L_S the latent heat of solidification (J/m^3), dfs/dt the solidification rate (1/s), h_∞ the heat transfer coefficient (W/m^2°Cs), T the instantaneous temperature of the specimen, T_∞ ambient temperature and M the modulus of the specimen (m). Before and after solidification dfs/dt is zero. The heat transfer coefficient can be obtained from the numerical processing of the experimental cooling curves using Eq. 2.

$$h_\infty = -Cp^{V}\frac{M}{(T-T_\infty)}\frac{dT}{dt} \qquad (2)$$

Experimental cooling curve data were used to obtain h_∞ as a function of time for each specimen and these data were plotted and numerically fitted. An equation that describes the operating heat transfer coefficient as a function of time was obtained.

With regard to the micro modeling of the solidification kinetics, Table 2 shows the nucleation and growth equations used to calculate the solid fraction evolution for the two alloys under study. In the case of nodular iron, a value of N = 1 x 10^{14} nodules/m^3 was assumed for nucleation in order to obtain an acceptable agreement between the measured and simulated cooling curves. It was assumed that the growth kinetics of each eutectic sphere was controlled by the diffusion of carbon from the liquid to the graphite nodule through an intermediate austenite layer. It was supposed that the ratio of the radius of austenite, Rγ, to the radius of graphite R_G, remained constant at a value of 2.4 [18]. For eutectic gray iron, an instantaneous nucleation model [20] was used, where the number of nucleation sites depends on the cooling rate of the melt when it reaches the eutectic temperature upon cooling.

Table 2.- Nucleation and growth models used for the simulation

Eutectic Nodular Iron			Ref.
Nucleation	$N = 1 \times 10^{14}$	(m^{-3})	-
Growth	$\frac{dR\gamma}{dt} = 8x10^{-11}\frac{\Delta T}{R\gamma}$	(m/s)	19
Eutectic Gray Iron			
Nucleation	$Ns = 1x10^5 + 3.36x10^4(dT/dt)$	(m^{-2})	20
	$Nv = 2.54(Ns)^{3/2}$	(m^{-3})	19
Growth	$\frac{dR_E}{dt} = 1.6x10^{-8}(\Delta T)^2$	(m/s)	21

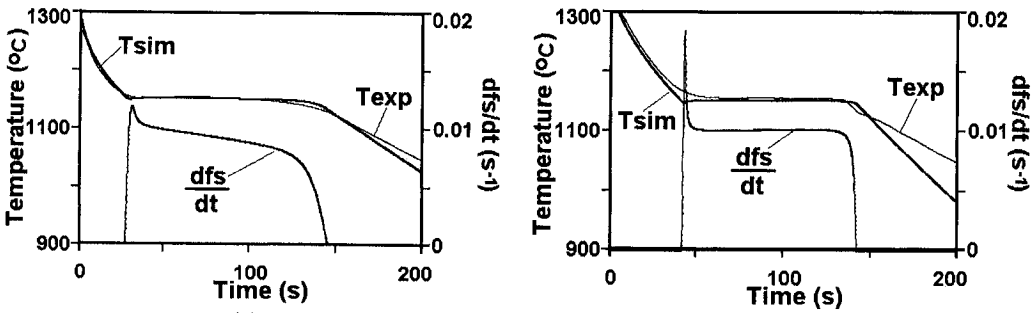

Figure 3. Simulated (Tsim) and experimental (Texp) cooling curves and NTA solidification rates (dfs/dt) of the simulated cooling curves for (a) Nodular iron; (b) Gray iron.

The eutectic cell growth model corresponds to the theory of cooperative irregular eutectic growth [13]. It assumes that the solid/liquid interface velocity follows a parabolic law as a function of the eutectic undercooling, ΔT (°C).

The simulated and the experimental cooling curves during solidification shown in Figure 3 have an acceptable agreement. The associated NTA solidification kinetics shows similar trends to those of the experimental curves.

Figure 4 shows the experimental and simulated solidification kinetics predicted by NTA for the nodular and the gray cast irons. The same general trends are observed after the initial stages of solidification in both cases. The nodular iron solidification rate decreases as the solidification

advances. The eutectic gray i
solidification process owing
eutectic growth mechanism. F
layer width increases as the s
liquid to the carbon nodule, w
continuously.

Finally it must be mentio
conditions has a good reprodu
tool for studying solidification

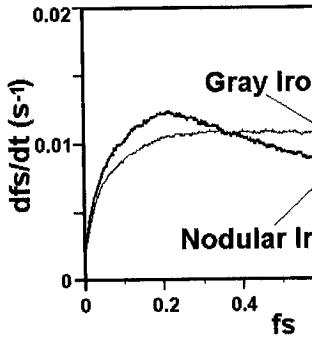

Figure 4. Solidification rates
for (a) experim

Figure 5. NTA Solidification

Summary

The NTA method detects dif
irons obtained from the sam
observations and NTA of s
kinetics model. NTA can be
further studies are needed to

Acknowledgements

The authors acknowledge the

as a function of time for each specimen
ation that describes the operating heat

kinetics, Table 2 shows the nucleation
lution for the two alloys under study. In
was assumed for nucleation in order to
nd simulated cooling curves. It was
s controlled by the diffusion of carbon
te austenite layer. It was supposed that
ite R_G, remained constant at a value of
nodel [20] was used, where the number
hen it reaches the eutectic temperature

ed for the simulation

	Ref.
(m^{-3})	-
(m/s)	19
t) (m^{-2})	20
(m^{-3})	19
(m/s)	21

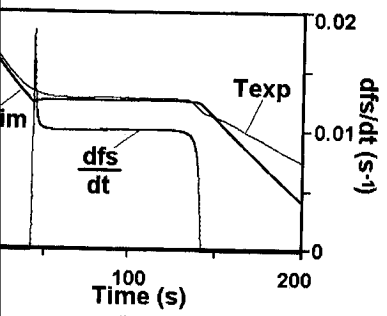

(b)

curves and NTA solidification rates
dular iron; (b) Gray iron.

ry of cooperative irregular eutectic
follows a parabolic law as a function

solidification shown in Figure 3 have
inetics shows similar trends to those

on kinetics predicted by NTA for the
observed after the initial stages of
rate decreases as the solidification

advances. The eutectic gray iron shows an almost constant solidification rate during most of the solidification process owing to the relatively less restricted nature of the cooperative irregular eutectic growth mechanism. For the nodular iron, the model shows that the intermediate austenite layer width increases as the solidification proceeds. This restricts the diffusion of carbon from the liquid to the carbon nodule, which explains why the solidification rate detected by NTA decreases continuously.

Finally it must be mentioned that the NTA method applied under controlled experimental conditions has a good reproducibility (see Fig. 5), which suggests that the NTA method is a useful tool for studying solidification kinetics.

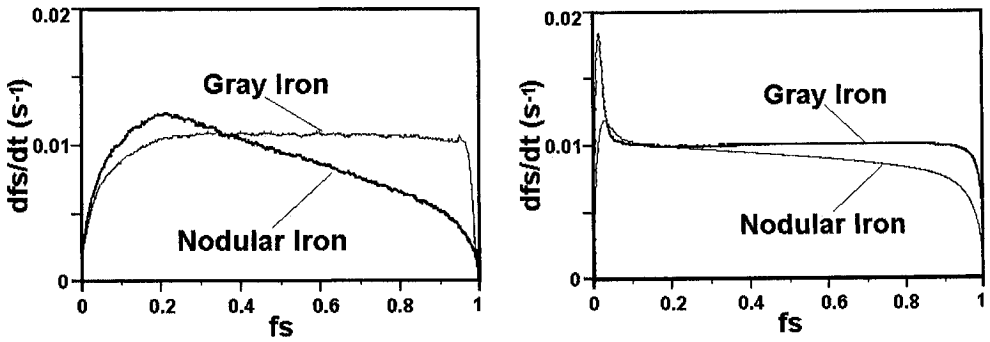

(a) (b)

Figure 4. Solidification rates (dfs/dt) as a function of the solid fraction (fs) for nodular and gray iron for (a) experimental cooling curves, and (b) simulated cooling curves.

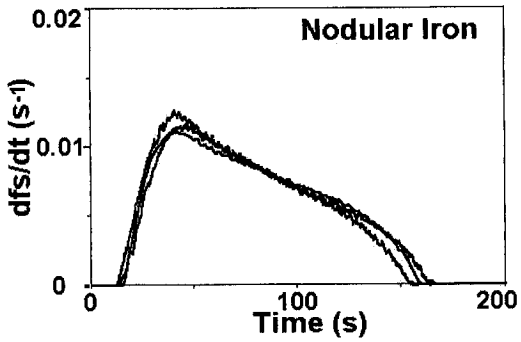

Figure 5. NTA Solidification rate evolution of eutectic nodular iron for three different experiments.

Summary

The NTA method detects differences of the solidification kinetics of near eutectic gray and nodular irons obtained from the same base alloy. This conclusion has been supported with metallographic observations and NTA of simulated cooling curves using a simple heat transfer solidification kinetics model. NTA can be a useful tool for qualitative studies of solidification kinetics, although further studies are needed to confirm the reliability of the method.

Acknowledgements

The authors acknowledge the financial support of DGAPA-UNAM and A. Amaro, I. Beltran, C.

Atlatenco, I. Puente, G. Gonzalez, S. García. and G. Aramburu for their heir valuable technical assistance

References

[1] E. Fras and W. Kapturckiewicz: AFS Transactions, Vol. 101 (1993), p. 505.

[2] C. González-Rivera, H. Cruz M., A. García and J. Juarez-Islas: J. Mater. Eng. Performance, Vol. 8.1, (1999) p. 103

[3] E. Fras and W. Kapturckiewicz: Met. and Mater. Trans. B, Vol. 28B (1997), p. 115.

[4] K. G. Upadhya, D. M. Stefanescu, K. Lieu and D. P. Yeager: AFS Trans., Vol. 97 (1989), p. 61.

[5] J. O. Barlow and D. M. Stefanescu: AFS Trans., Vol. 105 (1997), p. 349.

[6] W. T. Kierkus and J. H. Sokolowski: AFS Trans., Vol. 108 (1999), p. 161.

[7] S. L. Backerud and G. K. Sigworth: AFS Trans., Vol. 97 (1989), p. 459.

[8] C. Labrecque and M. Gagné: AFS Trans., Vol. 106 (1998), p. 459.

[9] D. Emadi and L. V. Whiting: AFS Trans., Vol. 110 (2002), p. 285

[10] R. J. Mac Kay, M. B. Djurdjevic and J. H. Sokolowsky: AFS Trans., Vol. 108 (2000), p. 521.

[11] M. Joaquim Oliveira, L. Filipe Malheiros and C. A. Silva Ribeiro: J. Mater. Proces. Tech., Vol. 92-93 (1999), p. 25.

[12] C. González-Rivera, J. Baez, R. Chavez, O. Alvarez and J. Juarez-Islas: Int. J. Cast Metal Res., Vol. 16 (2003),p. 531.

[13] P. Magnin: Acta Metall. Mater., Vol. 39 (1991), p. 469.

[14] D. Goettsch and J. Dantzig: Met. Mater. Trans. A, Vol. 25A (1994), p. 1063.

[15] G. L. Rivera, R. E. Boeri, J. A. Sikora: AFS Transactions Vol. 111 (2003), p. 979.

[16] M. I. Onsoien, O. Grong, O. Gundersen and T. Skaland: Met. Mater. Trans., Vol. 30A (1999), p. 1053.

[17] J. Lacaze, M. Castro and G. Lesoult: Acta Mater., Vol. 46 (1998), p. 997.

[18] F. J. Bradley: Scripta Metall., Vol. 25 (1991), p. 2091.

[19] E. Fras and H. López: Met. Mater. Trans. B, Vol. 30B (1999), p. 927.

[20] L. Nastac and D. M. Stefanescu: AFS Trans., Vol. 103 (1995), p. 329.

[21] A. Jacot, D. Maijer and S. Cockcroft: Met. Mater. Trans. A, Vol. 31A (2000), p. 2059.

Materials Science Forum Vol. 509 (M
online at http://www.scientific.net

Effect of Titanium ar

S. Sánchez[1,a], E. Ve

[1]Nem

[2]Doctorado en Ingeniería de

Autónoma de Nuevo León,

[a] samuel1408@hotma

Keywords: Fluidity, aluminun

Abstract. A series of tests ha
fluidity of liquid A319 and A
the A319 liquid alloy due to
particles increases the solid nu
increase of strontium, elimin
that titanium and strontium en
cast defects will be reduced. C

Introduction

Currently, the automobile ind
order to decrease production e
main alternatives under consi
advantages offered by this kin

There are several aspects
one of those. Some related op
machining, marketing and dis

Various processes and str
which are a common problem
of those strategies. The main
aluminum alloys A319 and
automotive parts.

Handling liquid alumin
fluidity of liquid metals for th
resistance of the fluid. Flow r
flow when a fluid layer of thi
moves to a velocity v [2]. A
interacting with the plates:

$$\tau = \eta\left(\frac{dv}{dh}\right) = \eta\dot{\gamma}$$

Where $\dot{\gamma}$ is the shear strain r
Newtonian fluids with a cons
related to the free volume, wh